Proceedings of the 21st ICSMGE, Vienna, Austria, 14 – 19 June 2026. Pistrol, Adam & Schweiger (eds.)
Published by: ÖGG, Austrian Society for Geomechanics, Salzburg, Austria, ISBN 978-3-9503898-4-5
https://doi.org/10.53243/ICSMGE2026-32

Reframing seismic vulnerability through the soil–structure interaction: Implications for existing and heritage buildings

María-Victoria Requena-García-Cruz, Antonio Morales-Esteban
Department of Building Structures and Geotechnical Engineering, University of Seville, Spain, mrequena1@us.es

ABSTRACT: Seismic vulnerability and loss analyses of buildings are typically conducted neglecting the influence of the soil-structure interaction (SSI). However, literature and past seismic events have demonstrated that the SSI can significantly affect the seismic response, particularly for mid- to high-rise buildings and heritage structures, particularly those founded on soft soils. This study investigates the impact of the SSI on the seismic performance and the expected losses of reinforced concrete (RC) buildings and heritage structures as case study buildings. Nonlinear static and dynamic analyses are performed within the OpenSees finite-element framework to assess their seismic behaviour. Two different SSI approaches are considered: the Beam on Nonlinear Winker method (BNWM) and the direct method. The findings reveal that accounting for the SSI significantly affects the fragility and the seismic performance of the buildings, with damage increasing by up to 38% due to the SSI. Additionally, the expected losses from both structural and non-structural damage are found to be notably higher when the SSI is considered. The findings highlight the importance of including the SSI in the seismic vulnerability assessments to improve the accuracy of seismic risk predictions and to ensure safer building design in seismically prone regions.

KEYWORDS: Soil-structure interaction; Seismic vulnerability; Loss assessment; Buildings; Nonlinear modelling.

1 INTRODUCTION

Seismic vulnerability assessments commonly idealize buildings as fixed-base systems, implicitly assuming that the foundation soil is rigid and that soil deformations do not influence the structural response. While this assumption simplifies modelling and has historically been considered conservative, extensive analytical, numerical, and experimental evidence has shown that SSI may either beneficially or detrimentally affect seismic performance, depending on soil conditions, foundation typology and structural characteristics (Kwag, Ju and Jung, 2018).

Recent earthquakes have further demonstrated that the SSI effects can amplify displacements, modify failure mechanisms, and increase damage concentrations, particularly for buildings founded on soft or medium-stiff soils (Liang et al., 2013). This is especially critical for existing RC buildings and heritage structures, which often exhibit limited ductility, poor detailing, significant irregularities and inadequate seismic design (Nuriga, Gidday and Lulseged, 2025). In such systems, SSI may interact with second-order (P–Δ) effects, masonry infill behavior and material degradation, leading to non-conservative vulnerability estimates if neglected (Dutta, Bhattacharya and Roy, 2004).

Although modern seismic codes acknowledge the relevance of the SSI for certain structural typologies, practical guidance for its quantitative inclusion in vulnerability and loss analyses remains limited. Consequently, SSI is often omitted in large-scale risk studies and even in detailed assessments of individual buildings. This paper addresses this gap by reframing seismic vulnerability through explicit consideration of SSI, focusing on its implications for both modern RC and heritage buildings.

2 BACKGROUND AND STATE OF THE ART

2.1 *The SSI phenomenon*

SSI arises from the mutual interaction between the deformable soil, the foundation system, and the superstructure. During seismic excitation, soil alters the input motion at the foundation level (kinematic interaction) and allows additional displacements and rotations due to foundation deformability (inertial interaction). These mechanisms modify the dynamic properties of the system, including natural periods, damping, and mode shapes.

2.2 *Modelling approaches for SSI*

Several modelling strategies exist to incorporate SSI in seismic analyses, ranging from simplified to highly detailed approaches (Vicencio, Alexander and Saavedra Flores, 2023). Among the most widely used are: i) Lumped-parameter and Winkler-based models, where soil flexibility is represented through nonlinear springs; ii) Macro-element approaches, which soil–foundation behavior into a limited number of degrees of freedom; and iii) Direct methods, in which soil, foundation and structure are modelled simultaneously using finite elements (FE).

The Beam on Nonlinear Winkler Method (BNWM) remains popular in engineering practice due to its relative simplicity and computational efficiency. It allows modelling of soil nonlinearity through p–y, t–z, and q–z springs and was validated against experimental data for shallow and deep foundations. Conversely, direct modelling approaches provide a more comprehensive representation of soil behaviour, including stress redistribution and 3D effects, but at a higher computational cost.

Recent studies highlighted that simplified SSI models may either underestimate or overestimate damage if soil properties and foundation details are not properly characterized (Requena-Garcia-Cruz et al., 2022). In particular, linear soil assumptions or overly coarse meshes in direct models can lead to results similar to fixed-base analyses, omitting potentially detrimental SSI effects.

2.3 *SSI and seismic vulnerability of existing buildings*

Existing reinforced concrete (RC) buildings constructed before the adoption of modern seismic codes often exhibit poor detailing, smooth reinforcement bars, weak columns, soft-storey mechanisms, and strong beam–weak column joints. Heritage structures, including masonry and mixed systems, present additional vulnerabilities due to material degradation, low tensile strength, and construction irregularities.

For these building classes, SSI may significantly alter damage distribution and failure modes. Increased flexibility at the foundation level may concentrate damage in already vulnerable storeys or structural elements, leading to earlier onset of significant damage or near-collapse conditions. Despite this, SSI is rarely considered in vulnerability and loss assessments of existing and heritage buildings, motivating the present study.

3 CASE STUDY

3.1 *Buildings under study*

The primary RC case study considered is representative of high-rise infilled buildings constructed in southern Europe during the mid-twenties. In this case, it is located in Seville (Spain). Such buildings typically feature irregular story heights (including soft-story mechanisms), low quality of structural materials and limited seismic detailing (Figure 1). In southern Spain, they are generally located over soft alluvial strata. As a result, these characteristics make them particularly sensitive to SSI effects.

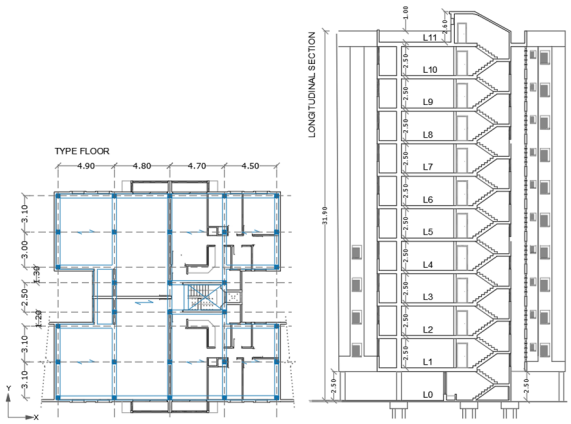

Figure 1. Configuration of the RC building. Elaborated by the authors.

To extend the discussion beyond RC buildings, a heritage structure archetype is also considered: the Mosque-Cathedral of Córdoba (Spain) (Figure 2). Apart from its value and being one of the UNESCO World heritage sites, this building reflects common features of historic buildings, such as masonry walls, flexible diaphragms and shallow foundations. While the numerical modelling strategy differs from RC frames, the influence of SSI on global performance and damage accumulation is assessed using similar performance metrics.

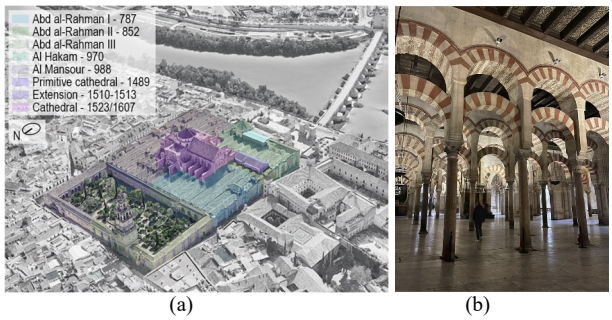

(a) (b)

Figure 2. (a) Mosque-Cathedral of Córdoba with extensions. (b) Interior view of the Abd 'al-Rahman I sector, with the coffered ceiling and the double horseshoe arches. Elaborated by the authors.

3.2 *Soil characterization*

The soil profiles considered are representative of the alluvial deposits commonly found in urban areas of the Guadalquivir valley, particularly in the cities of Seville and Córdoba (Figure 3). These deposits originate from fluvial sedimentation processes associated with the Guadalquivir River during the Quaternary period and form a strip approximately 4 km wide along the river course. The typical stratigraphic sequence consists of a basal granular layer of sandy gravels (thicknesses from 3-6 m), overlain by alternating layers of sands, silts and brown clays. At the surface, an anthropogenic layer associated with urban occupation is present (1-4 m thicknesses). The sequence is underlain by the Tertiary blue Guadalquivir marls, which act as seismic bedrock at depths between 10 and 18 m.

Geotechnical characterization is based on in-situ investigations, including Standard Penetration Tests (SPT) and two-dimensional Multichannel Analysis of Surface Waves (MASW), complemented by laboratory testing. The shear wave velocity (V_s) profile is adopted as the reference parameter for defining the remaining mechanical properties through established empirical correlations (Figure 3). The groundwater table is located at around 18 m depth. Hence, undrained conditions are assumed for short-term seismic loading in cohesive soil layers.

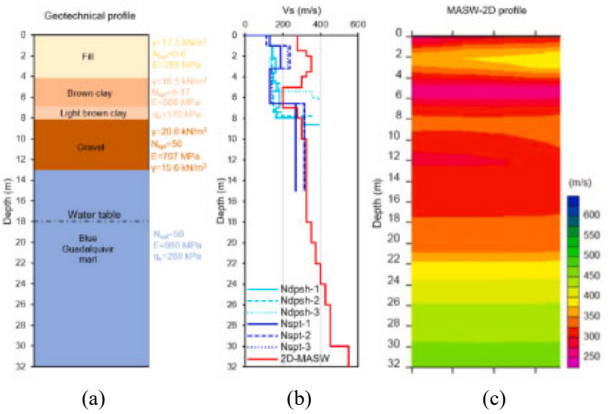

(a) (b) (c)

Figure 3. (a) Geotechnical profile from a nearby borehole. (b) V_s profile derived from in-situ testing results. (c) 2D-MASW profile near the northern wall of the Mosque-Cathedral. Elaborated by the authors.

3.3 *Seismic action*

Southern Spain is affected by both distant offshore seismic sources with long return periods and moderate-magnitude earthquakes occurring at relatively short distances. Regional seismicity is governed by the interaction between the Eurasian and African plates, which generates large offshore events near the Gorringe Bank and Cape St. Vincent, as well as moderate intraplate seismicity within the Iberian Peninsula (Fazendeiro Sá, Morales-Esteban and Durand Neyra, 2020).

A probabilistic seismic scenario corresponding to a return period of 475 years is adopted for both nonlinear static and dynamic analyses. The seismic action is defined using the spectral acceleration (S_A), with a reference peak ground acceleration (PGA) of 0.09g from the updated Spanish seismic hazard maps. The response spectrum is defined according to Eurocode 8-Part 1 (EC8-1) (CEN, 2004) for each soil class.

Ground motion (GM) records are selected from the European strong motion database (Luzi et al., 2020) based on their compatibility with the EC8 design spectrum for the site. The selection and scaling procedure follows the method proposed by (Morales-Esteban et al., 2012).

Figure 4 shows the selected GM for soil types A and C, together with the corresponding mean spectra and standard deviation.

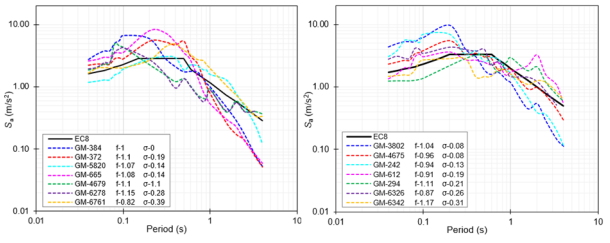

(a) (b)

Figure 4. GM considered for soil type A (a) and C (b) for a return period of 475 years. Note: standard deviation (σ) and factor of scale (f).

4 NUMERICAL MODELLING FRAMEWORK

4.1 *Superstructure modelling*

Nonlinear FE numerical models of the superstructures are developed within the OpenSees (McKenna, Fenves and Scott, 2000) and the STKO (Petracca, Candeloro and Camata, 2017). For the RC case study, 3D models are assembled using distributed plasticity beam–column elements with fibre-based cross-sections. This formulation allows explicit representation of concrete cracking and crushing, reinforcement yielding, confinement effects, and progressive stiffness degradation under cyclic loading. Masonry infills are modelled using equivalent diagonal struts with nonlinear hysteretic behavior, accounting for openings and post-cracking degradation.

For the heritage structure, a macro-mechanical modelling approach is adopted. Masonry walls, piers, and arches are discretised using solid elements governed by a damage–plasticity constitutive law capable of reproducing distinct tensile cracking and compressive crushing mechanisms (Petracca et al., 2017). This approach enables the simulation of stiffness degradation, irreversible damage accumulation, and strength loss, which are critical for assessing seismic performance in historic masonry systems. A mesh sensitivity analysis is carried out in all cases. Model calibration is supported by ambient vibration measurements and operational modal analysis (OMA). Further description on the procedure can be found in the previous work developed by the authors (Requena-Garcia-Cruz et al., 2023).

4.2 *SSI modelling strategies*

SSI is incorporated using two approaches that increase modelling fidelity. Both are compared against a fixed-base (FB) model to isolate the SSI effects.

The first approach is based on the BNWM (Figure 5), in which soil flexibility is represented by nonlinear springs acting in the horizontal and vertical directions at the foundation level. The springs follow established *p–y*, *t–z*, and *q–z* relationships (uniaxial materials 'PySimple', 'TzSimple1' and 'QzSimple1' in OpenSees, respectively) and are calibrated using site-specific geotechnical properties and established geotechnical formulations. These materials are later applied to the direction considered by using the 'zerolengthMaterial'. The behaviour of these materials is presented as a backbone curve with an initial elastic behaviour ending in a soft nonlinear behaviour. Alternative BNWM configurations are considered to investigate the influence of foundation idealization, including models with concentrated soil springs directly connected to the superstructure nodes and models with explicit representation of footing elements.

The second approach employs a direct modelling strategy, in which the soil domain, foundation system, and superstructure are modelled as a single coupled 3D FE system (Figure 6). The soil is discretized using solid elements governed by an elasto-plastic constitutive law suitable for undrained cohesive soils ('PressureIndependMultiYield' (PIMY) material), enabling simulation of nonlinear stress–strain behavior and hysteretic energy dissipation. The depth and lateral extent of the soil domain are selected to minimise boundary effects, and the bedrock is explicitly represented. Although computationally demanding, this approach provides a benchmark for evaluating the accuracy of simplified SSI formulations. Further description on the constitutive law model used in this model can be found in the previous work developed by the authors (Requena-Garcia-Cruz et al., 2022). In the case of the Mosque-Cathedral, in total, the FE mesh of the complete system is composed of 2,030,786 solid tetra elements and 335,671 nodes.

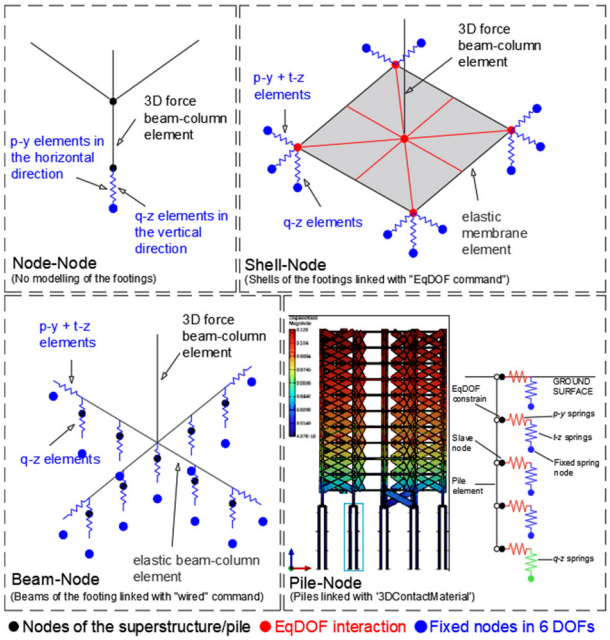

Figure 5. BNWM modelling approaches.

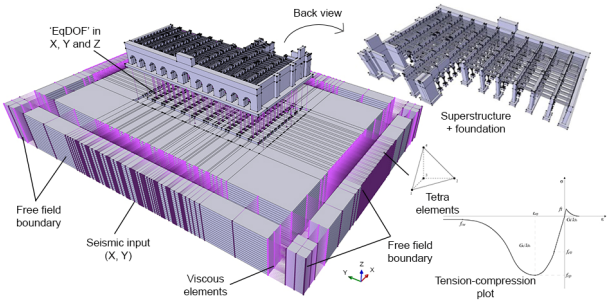

Figure 6. 3D FE model of the Abd al-Rahman I sector, including the foundation and the soil.

The definition of the geotechnical model is based on experimental measurements. Linear site response analyses have been carried out to determine the main resonance frequencies of the soil deposit in free field conditions. The depth of the soil in the numerical model extends down to the Blue Guadalquivir marl, i.e. the bedrock. In Table 1, the mechanical properties required for the numerical simulations are listed.

Table 1. Mechanical properties of the soil required for the numerical simulations. ρ, density of the materials; E, Young's modulus; G, shear modulus; B, bulk modulus; c, cohesion; ν, Poisson's ratio.

Material	Thickness	ρ	V_s	E	G	B	c	ν
	[m]	[T/m^3]	[m/s^2]	[GPa]	[GPa]	[MPa]	[kPa]	
Fill	0-4.2	1.78	250	289	111	241	30	0.3
Brown clay	4.2-7.35	1.78	350	568	218	473	50	0.3
Light brown clay	7.35-8.1	1.70	350	551	212	459	50	0.3
Gravel	8.1-13.9	2.10	360	707	272	589	150	0.3
Blue Guadalquivir marl	13.9-18	1.94	360	627	251	418	300	0.25
Blue Guadalquivir marl	18-22	1.94	450	980	392	653	300	0.25

4.3 *Analysis procedures*

Seismic response is evaluated through a combination of nonlinear static (pushover) (NLSA) analyses and nonlinear dynamic analyses (NLDA) using spectrally compatible ground motion records (selected in Figure 4). NLSAs are performed to derive capacity curves, which are subsequently transformed into equivalent single-degree-of-freedom (SDOF) systems following the N2-method as in EC8-1. Performance and

fragility are assessed at multiple damage limit states (DLs), including light damage (DL1), damage limitation (DL2), significant damage (DL3), and near-collapse (DL4), consistent with performance-based seismic assessment frameworks. The seismic safety is evaluated following the capacity/demand ratio (CDR) established in the EC8-3 (CEN, 2005), computed as the ratio between the LS considered and the seismic demand (D_{tb}). Drift-based fragility functions have been defined to estimate the damage in the structural and non-structural components according to (Aslani and Miranda, 2005) and (Cardone and Perrone, 2015), respectively. Damage to acceleration-sensitive non-structural components has been defined according to HAZUS (Federal Emergency Management Agency (FEMA), 2018). Further information on the procedure followed is presented in (Requena-Garcia-Cruz et al., 2022).

Nonlinear dynamic analyses are performed to capture cyclic degradation, higher-mode effects, and record-to-record variability, providing a robust basis for fragility and loss assessment. Demand parameters such as interstorey drift ratios (IDR), chord rotations, and acceleration demands are extracted and used to evaluate structural and non-structural damage.

4.4 *Loss analysis*

The total expected loss (E[Loss $_T$|IM]) as a function of the ground motion intensity (IM) has been calculated as the sum of: i) the losses resulting from the collapse of the building; ii) the losses due to the repairs, considering that the building has not collapsed; and, iii) losses due to the demolition of the building due to excessive residual drifts. Also, the probability of collapse that the structure will have for a certain IM has been accounted for as well as the probability that the structure will have to be demolished if it has not collapsed for a certain IM. Further information on the procedure can be found in (Requena-Garcia-Cruz, Romero-Sánchez and Morales-Esteban, 2022).

5 SEISMIC PERFORMANCE AND FRAGILITY ASSESSMENT

5.1 *Dynamic characteristics*

The inclusion of SSI systematically increases the fundamental periods of the analyzed structures and modifies modal participation. While mode shapes remain qualitatively similar, the interaction with deformable soil leads to period elongation and additional damping, which significantly influences displacement demand. As expected, softer soil profiles produce larger period shifts, confirming the sensitivity of the global dynamic response to soil flexibility.

Although direct comparison between fixed-base and SSI-including periods is not strictly meaningful due to the different mass and boundary conditions, the observed trends confirm that SSI has been properly captured and that dynamic behavior may differ substantially when soil compliance is considered.

5.2 *Capacity and damage mechanisms*

SSI models exhibit reduced initial stiffness and lower maximum base shear capacity compared to fixed-base configurations. Reductions in global capacity of approximately 15–20% are observed, depending on soil stiffness and modelling approach (Figure 7). This reduction is accompanied by increased displacement demand, leading to earlier activation of nonlinear mechanisms.

Damage tends to concentrate in already vulnerable structural components. In the RC building, SSI amplifies interstorey drift demands at the lower storeys, intensifying soft-storey mechanisms and increasing the likelihood of column failure. For the heritage structure, SSI leads to a broader spatial distribution of damage, extending from the base of perimeter walls to arches and upper wall sections. These effects are consistent with the performance indicators obtained, which predict more severe damage states when SSI is included.

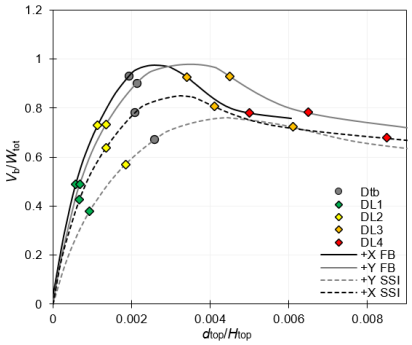

Figure 7. SDOF-NLSA normalized curves with DLs and seismic demand (D_{tb}) for the RC FB and the SSI models in the X and Y direction. Curves are normalized by the total shear base (V_b) and weight (W_{tot}) of the structure and by the displacement of the control node at the roof (d_{top}) and the total height (H_{top}).

5.3 *Interstorey drifts*

Based on the IDR limits proposed by the literature (D'Ayala et al., 2012), no damage is expected from the third storey up to the roof, as IDR values remain below 1.5–2% (DL2) (Figure 8). However, severe damage is expected at the first and second storeys, where IDR values range between 2.5% and 4%. At the ground storey, IDR exceeds 4%, indicating a high likelihood of column failure and potential local collapse.

When SSI is considered, drift demand increases significantly. At the ground storey, IDR values increase by up to 22%, further aggravating soft-storey mechanisms. In the upper storeys, from the third level to the roof, IDR values increase by up to 40%, leading to the development of light damage where none was previously expected under FB assumptions. These results confirm that SSI amplifies displacement demand and alters the vertical distribution of damage.

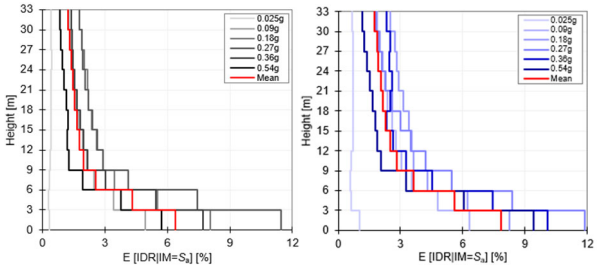

Figure 8. IDR as a function of height for the (a) FB and (b) SSI models

5.4 *Damage plots*

For the Mosque–Cathedral, damage concentration intensifies when SSI is included. In the FB model, damage is primarily localised at the lower sections of the perimeter walls and at the junction between the arcades and the northern wall. When SSI is considered, damage extends to the initial rows of arches and to the upper portion of the northern wall, indicating a wider spatial distribution of damage (Figure 9).

In terms of seismic demand displacement, the expected performance level lies between DL2 and DL3 for both FB and SSI models. However, the seismic safety ratio increases when SSI is included. For the FB model, this ratio is equal to 1.13 and 1.10 in the X (North–South) and Y (East–West) directions, respectively, whereas for the SSI model it increases to 1.36 and 1.25.

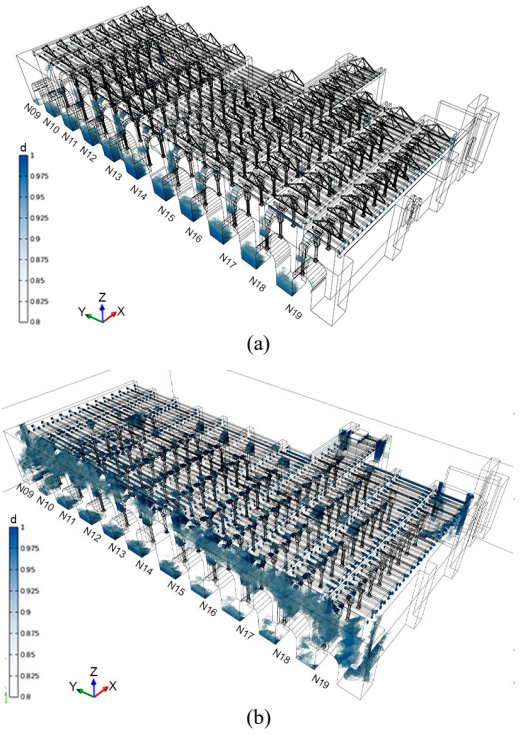

Figure 9. Damage plots in tension for the FB (a) and the SSI (b) models. Load applied in the X (North-South) direction.

5.5 *Fragility curves*

Fragility analyses reveal a systematic shift towards higher probabilities of reaching significant damage and near-collapse states when SSI is considered. For the analysed case studies, the probability of significant damage increases by up to 38% at the same intensity measure level compared to FB assumptions.

Fragility curves are derived considering the seismic demand displacement obtained from the N2-method. As shown in Figure 10, RC SSI-models consistently exhibit worse fragility performance than their fixed-base counterparts, resulting in higher probabilities of exceeding each damage state. Focusing on the near-collapse limit state, the probability associated with the expected seismic demand increases by up to 20% in the X direction (from 65% to 78%), while in the Y direction an increase of up to 11% is observed.

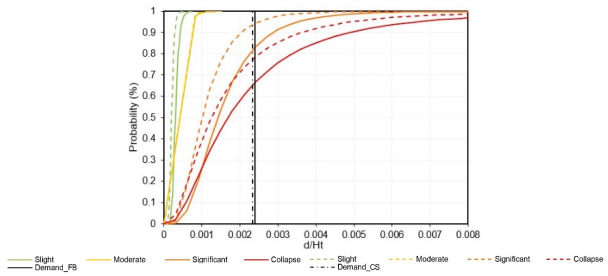

Figure 10. Fragility curves for the RC FB (continuous) and SSI (dash) models in the X direction.

6 IMPLICATIONS FOR SEISMIC LOSS ASSESSMENT

The explicit inclusion of the SSI has a pronounced impact on seismic loss estimates for existing buildings. The increase in displacement demand and damage probabilities observed in SSI-models directly translates into higher expected economic losses across all IM levels.

Loss curves show that, for a given GM intensity, SSI-models consistently yield higher expected losses than FB configurations. This increase is mainly driven by higher probabilities of reaching moderate to severe damage states, which govern repair and replacement costs. Drift-sensitive non-structural components, such as masonry infills, represent the dominant contribution to expected losses, while acceleration-sensitive components contribute marginally.

The expected (mean) losses have been expressed, for the different elements, for the near collapse damage state, $E[L_j|NC,IM]$. For the RC case study, at the design ground acceleration level of 0.09g, expected losses increase from 0.07% of the replacement cost in the FB model to 0.17% when SSI is considered, corresponding to an increase of approximately 140% (Figure 11). Structural damage constitutes a significant portion of the total losses. However, non-structural drift-sensitive components remain the primary drivers of economic impact.

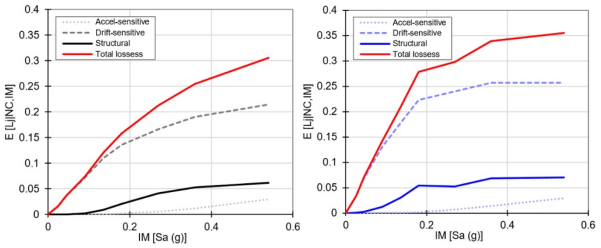

Figure 11. Loss curves considering the structural and non-structural acceleration and drift-sensitive components for the RC FB (a) and SSI (b) models, respectively.

7 DISCUSSION

The results confirm that the SSI has a significant influence on the seismic vulnerability and loss estimation of existing RC and heritage buildings, and should not be treated as a secondary effect. Contrary to the common assumption that SSI is inherently beneficial due to period elongation, the findings show that SSI may amplify displacement demand, intensify damage concentration, and increase the probability of reaching severe damage and near-collapse states, particularly for structures founded on soft or medium-stiff soils.

The comparison between simplified BNWM approaches and the direct soil–foundation–structure modelling indicates that, when properly calibrated, simplified SSI models are capable of capturing the main trends observed in more detailed analyses. However, inadequate soil characterization or oversimplified soil behaviour may mask detrimental SSI effects, leading to non-conservative assessments.

For the RC case study, SSI amplifies soft-storey effects and concentrates damage at lower levels, with interstorey drifts increasing by up to 22% at the ground floor and up to 40% in upper storeys. This explains the observed increase in the probability of significant damage and near-collapse. In the heritage structure, SSI alters the spatial distribution of damage, extending it to upper walls and arch systems that remain largely unaffected in FB models. These results indicate that FB assumptions may omit critical vulnerability patterns, particularly in masonry heritage buildings.

The impact of SSI on loss estimation is substantial. Expected losses increase significantly when SSI is considered, with values up to 140% higher at the design PGA level. Drift-sensitive non-structural components, especially masonry infills, dominate the loss contribution, highlighting the limitations of conventional loss models based on FB fragility functions. Neglecting SSI may therefore bias retrofit prioritization, emergency planning, and risk mitigation strategies, particularly in historic urban areas founded on soft soils.

From a risk-informed perspective, neglecting SSI can significantly underestimate both damage and expected losses, potentially biasing retrofit prioritisation, emergency planning, and resource allocation. This is particularly critical for heritage structures, where SSI may contribute to irreversible damage and loss of cultural value. The results highlight the need to explicitly account for SSI in performance-based seismic assessments of existing and heritage buildings located in urban areas with unfavourable soil conditions.

8 CONCLUSIONS

This study demonstrates that the SSI plays a critical role in the seismic vulnerability and loss assessment of existing buildings. The main conclusions of this work are the following:

1. Accounting for SSI leads to systematic increases in fundamental periods and displacement demand, modifying the global seismic response.
2. For the case study buildings on soft alluvial strata, SSI-models exhibit reduced stiffness and capacity, with damage concentrating earlier in vulnerable structural components.
3. Fragility analyses show increased probabilities of significant damage and near-collapse, with increases of up to 38% compared to fixed-base assumptions.
4. Expected economic losses are significantly higher when SSI is considered, with increases of up to 140% at the design ground motion level, mainly driven by drift-sensitive non-structural components.
5. Heritage structures are particularly sensitive to SSI, as foundation flexibility alters damage distribution and affects architecturally significant elements.
6. Simplified SSI models, such as BNWM, can provide reliable results when properly calibrated, offering a practical alternative to computationally demanding direct methods.

Overall, the findings demonstrate that neglecting the SSI may lead to non-conservative seismic risk estimates. Explicit consideration of the SSI is essential to improve the reliability of seismic vulnerability and loss assessments and to support informed decision-making for the protection and retrofit of existing and heritage buildings in seismic-prone regions.

9 ACKNOWLEDGEMENTS

This manuscript is part of the R + D + i project “Metodología avanzada para la evaluación de la seguridad estructural y sísmica de edificios patrimoniales”. Grant “Proyecto PID2023-150771OB-I00” funded by “MCIN 10.13039/501100011033” and by the “European Union”. The authors would like to thank the Cathedral of Córdoba's Chapter for the support and for enabling the study of the monument.

10 REFERENCES

Aslani, H. and Miranda, E., 2005. Probabilistic earthquake loss estimation and loss disaggregation in buildings. Department of Civil and Environmental Engineering, Stanford University, CA 94305-4020. (157), p.383.

Cardone, D. and Perrone, G., 2015. Developing fragility curves and loss functions for masonry infill walls. *Earthquake and Structures*, 9(1), pp.257–279. https://doi.org/10.12989/eas.2015.9.1.257.

CEN, 2004. *Eurocode 8: Design of structures for earthquake resistance. Part 1: General rules, seismic actions and rules for buildings*. Brussels, Belgium.

CEN, 2005. *Eurocode-8: Design of structures for earthquake resistance. Part 3: Assessment and retrofitting of buildings*. Brussels, Belgium.

D’Ayala, D., Kappos, A., Crowley, H., Antoniadis, P., Colombi, M., Kishali, E., Panagopoulos, G. and Silva, V., 2012. *Providing building vulnerability data and analytical fragility functions. U.S. Geological Survey Under the National Earthquake Hazards Reduction Program*, .

Dutta, S.C., Bhattacharya, K. and Roy, R., 2004. Response of low-rise buildings under seismic ground excitation incorporating soil-structure interaction. *Soil Dynamics and Earthquake Engineering*, 24(12), pp.893–914. https://doi.org/10.1016/j.soildyn.2004.07.001.

Fazendeiro Sá, L., Morales-Esteban, A. and Durand Neyra, P., 2020. Regional correlations for estimating seismic amplification. Implications for loss assessment in SW Iberia. *Soil Dynamics and Earthquake Engineering*, 130. https://doi.org/10.1016/j.soildyn.2019.105993.

Federal Emergency Management Agency (FEMA), 2018. *Earthquake Loss Estimation Methodology (HAZUS) software*.

Kwag, S., Ju, B.S. and Jung, W., 2018. Beneficial and Detrimental Effects of Soil-Structure Interaction on Probabilistic Seismic Hazard and Risk of Nuclear Power Plant. *Advances in Civil Engineering*, 2018. https://doi.org/10.1155/2018/2698319.

Liang, J., Fu, J., Todorovska, M.I. and Trifunac, M.D., 2013. Effects of site dynamic characteristics on soil-structure interaction (II): Incident P and SV waves. *Soil Dynamics and Earthquake Engineering*, 51, pp.58–76. https://doi.org/10.1016/j.soildyn.2013.03.003.

Luzi, L., Lanzano, G., Felicetta, C., D’Amico, M.C., Russo, E., Sgobba, S. and Pacor, F., 2020. *Engineering Strong Motion Database (ESM) (Version 2.0)*. [online] Istituto Nazionale di Geofisica e Vulcanologia (INGV). https://doi.org/10.13127/ESM.2.

McKenna, F., Fenves, G.L. and Scott, M.H., 2000. *OpenSees: Open system for earthquake engineering simulation. Pacific Earthquake Engineering Research Center*. [online] Berkeley, CA: University of California. Available at: <https://opensees.berkeley.edu/> [Accessed 21 November 2019].

Morales-Esteban, A., de Justo, J.L., Martínez-Álvarez, F. and Azañón, J.M., 2012. Probabilistic method to select calculation accelerograms based on uniform seismic hazard acceleration response spectra. *Soil Dynamics and Earthquake Engineering*, 43. https://doi.org/10.1016/j.soildyn.2012.07.003.

Nuriga, M.A., Gidday, B.G. and Lulseged, A., 2025. Impact of soil-structure interaction on seismic performance: a comparative analysis across varied soil conditions. *Innovative Infrastructure Solutions*, 10(10), p.470. https://doi.org/10.1007/s41062-025-02268-4.

Petracca, M., Candeloro, F. and Camata, G., 2017. *‘STKO user manual’. ASDEA Software Technology*. [online] Pescara, Italy. Available at: <https://asdeasoft.net/pdf/STKOUserManual.pdf> [Accessed 8 July 2020].

Petracca, M., Pelà, L., Rossi, R., Zaghi, S., Camata, G. and Spacone, E., 2017. Micro-scale continuous and discrete numerical models for nonlinear analysis of masonry shear walls. *Construction and Building Materials*, 149, pp.296–314. https://doi.org/10.1016/j.conbuildmat.2017.05.130.

Requena-Garcia-Cruz, M.V., Bento, R., Durand-Neyra, P. and Morales-Esteban, A., 2022. Analysis of the soil structure-interaction effects on the seismic vulnerability of mid-rise RC buildings in Lisbon. *Structures*, 38, pp.599–617. https://doi.org/10.1016/j.istruc.2022.02.024.

Requena-Garcia-Cruz, M.V., Romero-Sánchez, E., López-Piña, M.P. and Morales-Esteban, A., 2023. Preliminary structural and seismic performance assessment of the Mosque-Cathedral of Cordoba: The Abd al-Rahman I sector. *Engineering Structures*, 291. https://doi.org/10.1016/j.engstruct.2023.116465.

Requena-Garcia-Cruz, M.V., Romero-Sánchez, E. and Morales-Esteban, A., 2022. Numerical investigation of the contribution of the soil-structure interaction effects to the seismic performance and the losses of RC buildings. *Developments in the Built Environment*, 12, p.100096. https://doi.org/10.1016/j.dibe.2022.100096.

Vicencio, F., Alexander, N.A. and Saavedra Flores, E.I., 2023. A State-of-the-Art review on Structure-Soil-Structure interaction (SSSI) and Site-City interactions (SCI). *Structures*, 56, p.105002. https://doi.org/10.1016/j.istruc.2023.105002.